# Virtual SEA – FEA-Based Modeling of Mid-Frequency Structure-Borne Noise

**Laurent Gagliardini** and **Laurent Houillon**, PSA-Peugeot-Citroen, Velizy-Vilacoublay, Cedex, France
**Gérard Borello**, InterAC, L'union, France
**Luca Petrinelli**, Geci Systèms, Versailles, France

**Virtual SEA (statistical energy analysis) is similar to experimental SEA, but based on frequency response functions computed using a FE model of the studied structure. The knowledge of the internal loss factors (defined by the user) as well as numerous observation and excitation points leads to a consistent data set that may be used to properly identify a SEA model. This process has been improved by developing an original automatic sub-structuring technique that guarantees optimized model construction and consequently a robust identification. This last feature supports SEA users with a lower level of expertise. As an example, virtual SEA is applied to the floor of a minivan. Convincing results are obtained when compared to experimental methods.**

Improvement in vehicle acoustic performance at low frequencies (booming noise) and high frequencies (insulation) has left perceived medium frequencies (200-1000 Hz) as the critical band in passenger comfort vs. power-train or road excitations. Simultaneously, new design processes (e.g. systems engineering), development time reduction and prototype availability are pushing computational methods, which can predict vehicle performances in any technical field – CFD and thermal comfort, durability, crash analysis, CEM, vehicle dynamics and NVH. Sound transmission at medium frequencies (especially structure-borne transmission) is one of the last vibroacoustic subdomains not covered by any computational method.

This frequency range is part of the physical medium frequencies, where the response of the structure involves global as well as local behaviors. Neither the 'modal' behavior, dominant at low frequencies, nor the 'statistical' behavior, dominant at high frequencies, can alone represent the medium frequency behavior. Numerous dedicated computational techniques for addressing this issue are in progress and have remained at a research stage until now.[1-5]

Thus, the industrial design process led us to develop a method whose main features include adaptability to the current design process, reducing operating time, and lowering the required user level of expertise. The proposed method, called Virtual SEA, allows car body modeling that surpasses traditional SEA limitations by an extensive use of numerical simulation.[6-7]

This article covers the Virtual SEA method and includes an example application using the floor of a minivan (Peugeot 806). First, a brief background of the method is presented.

## Extension of the FEA Process to Medium Frequencies

With crash analysis, refined meshes such as the one shown in Figure 1 are available, at least for the body in white (BIW), from the early design stage of any vehicle project.

The mesh size of a few centimeters allows computations up to 1 kHz with no major difficulty. Because of insufficient memory size problems, a direct solver is used instead of the common modal solution. The resulting increase of the CPU time has not been seen as an obstacle, considering a number of recent improvements in numerical solvers for dynamic problems.[8-10]

If FE computations are available at rather high frequencies, why not use FEA directly?

- Increasing frequency makes the structures hyper-sensitive to small uncertainties in material properties and geometrical details. Such sensitivity, inherent to mass production objects such as cars, cannot be ignored in the medium frequency range. In this case only space- and frequency-averaged responses (i.e., energetic responses) can be predicted with adequate precision.
- FE modeling in itself does not provide the understanding necessary for project improvement. The modal understanding of the structure, used at low frequencies, is no longer relevant due to the high number of modes overlapping to produce the observed responses. Modal behavior provides clear design information through the locations of kinetic and elastic energies, respectively, indicating where mass and stiffness or damping modification are sensitive. At higher frequencies, when modes start overlapping, such information is no longer available. In the asymptotic case of high frequencies, the kinetic and elastic energies are considered equal at any point of the structure.

Figure 3 shows the comparison of computed and measured space and frequency averaged transfer functions between different parts of the minivan floor shown on Figure 2. The plot shows the matrix of energetic transfer functions defined as:

$$H_{ij} = \frac{\left\langle |\mathbf{v}|^2 \right\rangle_{\Delta f, \Omega_i}}{\mathrm{Re}\left\{ \left\langle \mathbf{v}_j^+ \mathbf{F}_j \right\rangle_{\Delta f} \right\}} \qquad (1)$$

where $\langle\ \rangle_{\Delta f}$ indicates a frequency average, and $\langle\ \rangle_{\Omega}$ a space average, and

$$P_i = \mathrm{Re}\left\{ \left\langle \mathbf{v}_j^+ \mathbf{F}_j \right\rangle_{\Delta f} \right\}$$

is the input power at the excitation point (superscript '+' indicates the conjugate transposed vector or matrix).

This quantity is preferred to the squared transfer of mobility function because its variance among input points is much smaller, meaning it provides more information about the dynamics of the system. Its use in the Virtual SEA Process is shown explicitly in the appendix.

Note that, although observation as well as excitation points do not have the same location in both cases, measurements and computations lead to very similar results in terms of spectral shape and spread among excitation points – except for part 1, where calculations show an overestimated value that was later related to a reinforcing plate, unfortunately welded to the prototype. This problem is purposely highlighted in order to emphasize the difficulties inherent in a design process. With the possibility of local changes in the body design, any modeling, even the most accurate, remains uncertain regarding the design process. Work is in progress in order to account for such modeling uncertainties.

Based on Paper #2003-01-1555, "Virtual SEA: Mid-Frequency Structure-Borne Noise Modeling Based on Finite Element Analysis," © 2003 SAE International, presented at the Noise & Vibration Conference, May 5-8, Traverse City, MI, 2003.

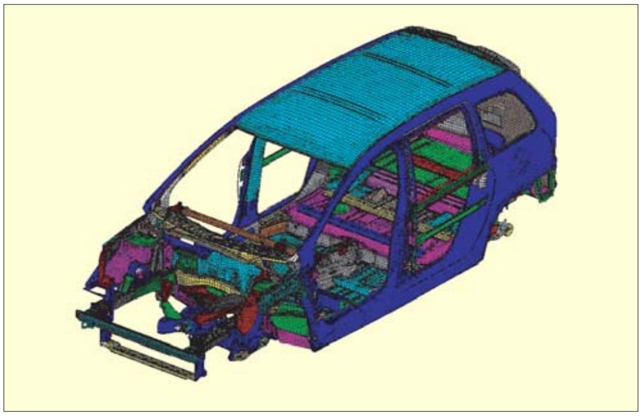

*Figure 1. Body In white of a 307 SW car.*

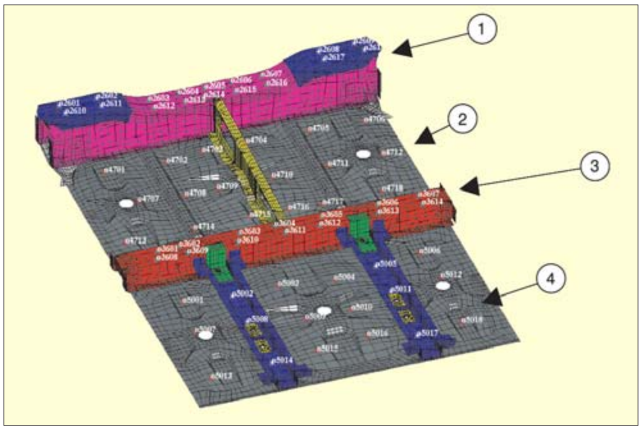


*Figure2. Front central part of a minivan floor structure defining 4 subsystems.*

## Limitations of Classical SEA

Looking at vehicle project issues (mainly trim design, but also vibration source strength specification), SEA appears to be a very convenient tool for the design stage of a project. It is widely used for air-borne transmission of sound, but some unexpected difficulties are arising with structure-borne sound. For example, most car body parts do not look like conventional structures such as flat plates, cylinders or beams. Moreover, when a candidate subsystem appears, its limits are difficult to draw, due to wired 3D-geometries.

For additional reasons, experimental SEA and analytical SEA cannot currently produce a robust car body SEA model in the target frequency range of 200-1000 Hz. Experimental SEA is limited by a lack of consistency in the measured data, but also because the sub-structuring is not controlled, which can lead to contradictory behaviors between points of the same subsystem. This sub-structuring problem is also encountered while building analytical SEA models. With analytical models, the user also has to tune the model to account for heterogeneity (e.g., corrugations, small hollow bodies, variable beam cross-sections, etc.). Overcoming these difficulties would require an impractically high level of expertise among all design engineers.

## Virtual SEA

From the mentioned difficulties, it was decided:

- To use finite elements to simulate a fully consistent energetic transfer function matrix measurement, and associated inputs.
- To look for the optimal gathering of observation/excitation points (sub-structuring process).
- To use an existing experimental SEA process to identify a SEA model.

Other models[11] have been considered but rejected at this stage, because they rely on a priori knowledge of the sub-structuring. Even when the method, currently referenced as Energy Influence Coefficients, provided an exact evaluation of the subsystems energy, there was critical lack of control on the sub-structuring.

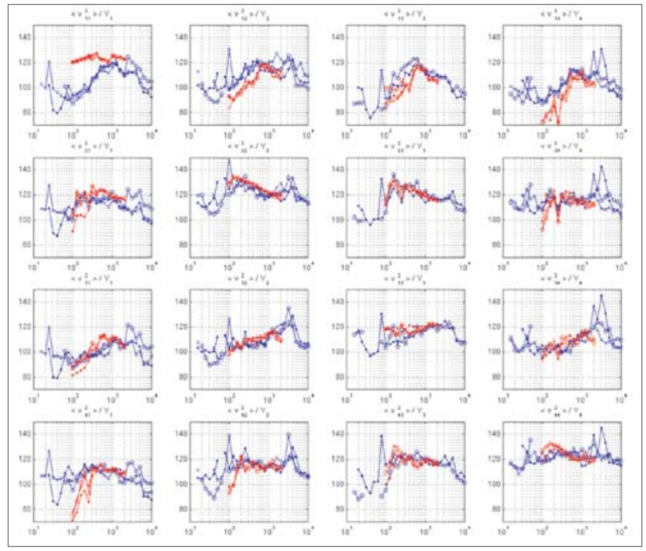

*Figure 3. Matrix of energetic transfer function between the 4 sub-systems as defined in Figure 2, computed (red – 100 Hz-2 kHz) and measured (blue – 20 Hz-10 kHz).*

**Energetic Transfer Functions Computation.** The first step is in our proposed method is a numerical experiment using FEA to compute frequency response functions. This approach relies on two different meshes. The first one is a refined mesh allowing FE computations up to 2 kHz, easily obtained because of its similarity to meshes used for crashworthiness studies. The second one, called "NVH mesh," is a coarse mesh extracted from the refined mesh providing a relevant sampling of the vibratory behavior of the structure. It contains several hundreds nodes and is used to estimate subsystems energies.

Damping is modeled through uniform structural damping, which could later be used as a SEA Damping Loss Factor. This damping will be close to the actual damping in case a later CLF (Coupling Loss Factor) evaluation would depend on damping.

Then, each node of the refined mesh, corresponding to the "NVH mesh" nodes, is successively excited by a unit force, normal to the structure, and the transfer functions are computed for all the nodes of the "NVH mesh." This simulation is performed using the Nastran V2001 direct solver on an IBM SP2 computer. The result of the simulation is a rectangular matrix of transfer functions between nodal normal unit loads, and 3 velocity DOFs at the observation points. This database is then compressed by a FORTRAN program to compute the input mobility and the Energetic Transfer Functions (Eq. 1). This new database is averaged over 1/3 octave bands.

**Automatic Sub-Structuring Process.** As soon as a database of point to point Energetic Transfer Functions is available, SEA analysis requires a compression of this information over a limited number of subsystems. This data reduction is the most critical phase of creating the SEA model. Past experimental SEA applications to car bodies have demonstrated the importance of a 'good' sub-structuring scheme.

When the database is compressed over an inappropriate sub-structuring scheme, the inverse problem that follows (see next paragraph and appendix) may result in a non-physical solution. These discrepancies are mainly due to some abusive weak coupling assumption between SEA subsystems. Unfortunately for a car body the "weak coupling assumption" is not intuitive and cannot be predicted until a clear definition exists.

From a practical point of view, FE generates a tremendous amount of data, and dividing that data into subsystems could become a very tedious and nearly impossible task without computer help. Thus, the process was automated based on the following principles:

- A subsystem is an energetic entity that must simultaneously exhibit a significant energy level difference with other sub-

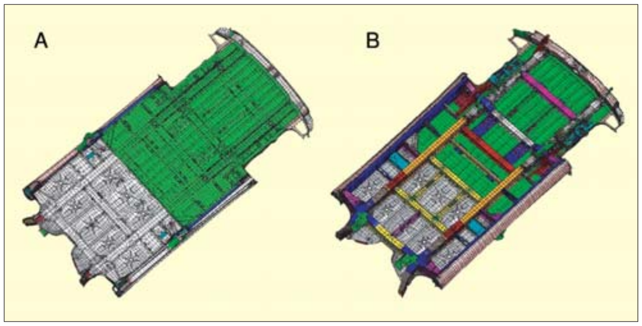


*Figure 4. Top (A) and bottom(B) views of a minivan floor structure mesh.*

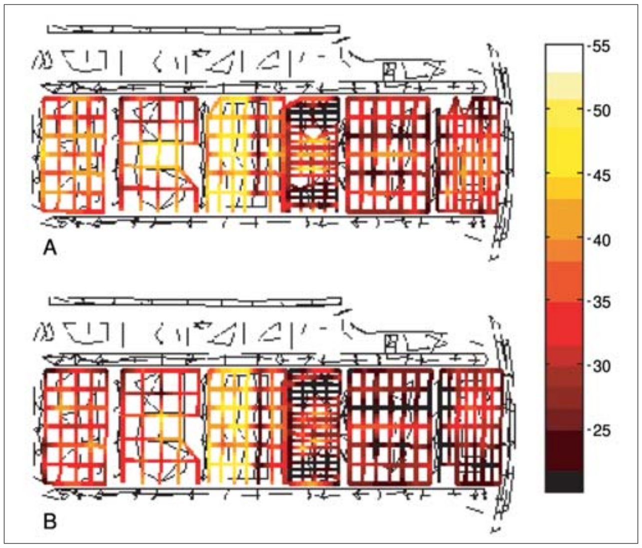


*Figure 5. One kHz, third octave averaged velocities map measured over the floor; bare (A) and trimmed (B).*

systems, and minimized internal heterogeneity.

- For any partition scheme, averaged responses and internal variances are used to compute the distance to the above ideal situation.
- The partition scheme is optimal when the distance is minimal.

An iterative algorithm was thus developed.

**Initialization.** The initializing sequence first creates a set of subsystems as follows:

1. An arbitrary excitation point is selected and a first set of points, with response lower than a given energy threshold, is retained.
2. These points are used as excitation points to create a new series of sets.
3. Reciprocity is then invoked to find strongly linked points.
4. These points are then isolated from the whole set of points; a new subsystem is then created.
5. The above sequence is reiterated and ends when all points have been affected to a subsystem.

At this stage a series of subsystem sets is available but the partition still needs to be improved.

**Optimization.** Different techniques have been tested to perform an optimization of the sub-structuring scheme:

- Statistical entropy techniques try to minimize an entropy function expressed under the generic following form, as defined in Shannon's theory of information:

$$H(G) = -\sum_n p_n \cdot \ln p_n \tag{2}$$

where $p_n$ is the probability of an event and $n$ the number of events. The events can be the point membership of a given set.

- Attraction force techniques rely on an attraction force between a point and a set of points; each point should belong to the most attractive set. The attraction force is expressed from the energetic transfer functions.

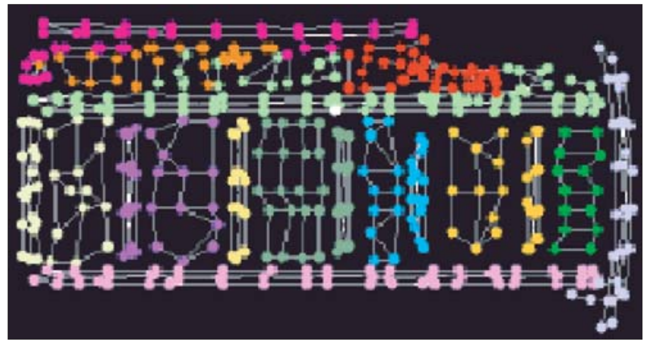

*Figure 6. Sub-structuring at 500 Hz.*

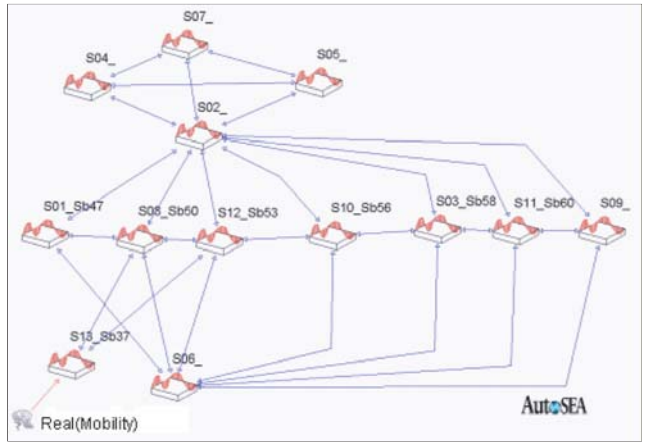


*Figure 7. AutoSEA1 model – result of the 500 Hz sub-structuring.*

In statistical entropy techniques, a point is moved randomly from one set to another until the entropy reaches a minimum; another point is then randomly chosen and the process is repeated as many times as necessary.

The attraction process works in a similar way, but faster, as a point can be moved from one set to another following maximum line forces. Unfortunately, this optimization process may never converge, and some of the points may remain definitely unstable. Further work is required to identify robust convergence criteria.

In practice, the iterative algorithms are improving the sub-structuring very rapidly and a subsystem set can be identified within a few minutes. Providing such an optimized sub-structuring scheme, independent of the user expertise, is a primary advantage of our proposed Virtual SEA method.

As the iterative algorithm relies on energetic transfer functions in a given frequency band (here 1/3rd octave), the sub-structuring process can be performed in each of the studied bands, leading to different sub-structuring schemes. It is remarkable that the number of subsystems increases with frequency as suggested by SEA assumptions on modal densities (increasing with frequency) or weak coupling conditions (also improving with frequency). From a practical point of view, it seems that the model range of validity is centered a few 1/3 octaves lower than the model optimization frequency.

## Inverse SEA Process

As soon as an appropriate data reduction is performed on the now defined subsystems, the coupling scheme and associated SEA parameters of the model can be identified.[13-16] The model identification is detailed in the appendix. The experimental SEA engine of the SEA-XP software[14] was used for this process.

The SEA-XP software, developed by InterAC to predict the energy transfer in a rocket engine at lift-off,[17] has been widely used by the automotive industry to validate SEA models of automobile bodies and rail cars.[18-19] It includes specific features required in complex structures such as a Monte Carlo matrix inversion and connection scheme design tool.

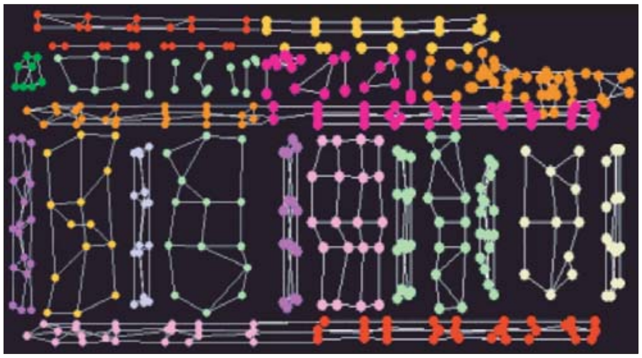

*Figure 8. Sub-structuring at 2 kHz.*

In practice, most of the automobile body structure is far from the homogeneous conditions ideally handled by theoretical SEA as input mobilities and transfer functions exhibit high degrees of spatial variance. The parametric identification of these high-variance SEA systems is thus performed in SEA-XP by a dedicated matrix solver; the Monte Carlo solver.

The Monte Carlo solver randomly perturbs energy matrices according to the variance of space- and frequency-averaged Energetic Transfer Functions, and filters out unwanted sets of equivalent mass and Coupling Loss Factors (non-physical negative values). This improves the identification process by considering possible data sets that are slightly different from the original, uncertain set. The connection scheme design is the iteration of two steps – selecting connection-involving power flow higher than a given threshold, and checking the quality of the associated identification process.

Finally, the resulting SEA model is described in a neutral file, including sub-structuring and connection schemes, equivalent masses and modal densities of subsystems, and Coupling Loss Factors. The Damping Loss Factor (DLF) is uniform and constant as it was in the computations. Actual values of damping are generally tuned and modified later as in any SEA application. SEA-XP can export created experimental models to AutoSEA in both version 1 and 2 format.

## Application: Minivan Floor

**Principles of the Application.** Virtual SEA has been applied to the floor structure of a minivan (See Figure 4). The numerical results have been compared to measurements and an AutoSEA2 model. Moreover, the effect of the trim on the floor structure has been modeled by modifying the DLF of the SEA subsystems touched by the trim. The results are also compared to the experiments.

The refined mesh of the minivan floor contains about 600,000 degrees of freedom, whereas the "NVH mesh" has only 500 nodes. The Transfer Functions have been computed at about 300 frequencies between 180 Hz and 2250 Hz, covering 1/3 octave bands between 200 Hz and 2 kHz.

**Measurements.** Experiments have been carried out with an artificial excitation (electrodynamic shaker) applied to the back hook supporting the exhaust line. Only the panels' vibration wase measured. A laser vibrometer scanning system was used to avoid adding sensors and the mass perturbations they cause at high frequencies (here above 1 kHz using standard equipment). At least 20 discrete points were measured on each panel, including stiffeners when they are part of the subsystems. The input mobility was also measured to compute the Energetic Transfer Functions.

Figure 5 shows measured velocity maps in the 1 kHz 1/3 octave band for the bare (A) and trimmed (B) floor. These measurements show how the trim influence decreases with frequency, interpreted as an effect of the decreasing coupling between the structure and the foam layer of insulation.

**Floor Structure.** As described in a previous paragraph, the Virtual SEA prototype software allows the user to perform the sub-structuring process in a particular 1/3 octave band. In the present case, two Virtual SEA models were computed to cover

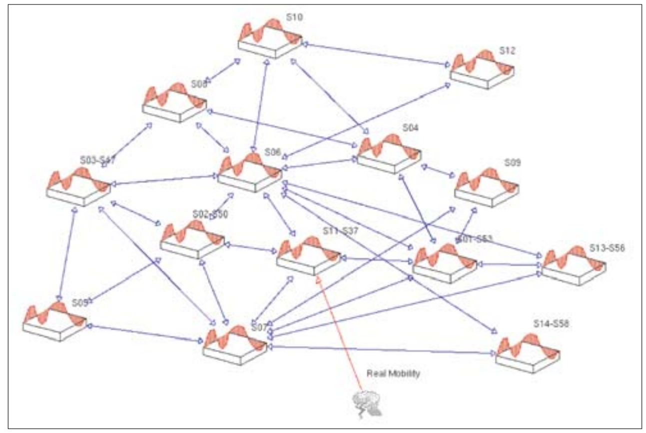


*Figure 9. AutoSEA1 model – result of 2 kHz sub-structuring.*

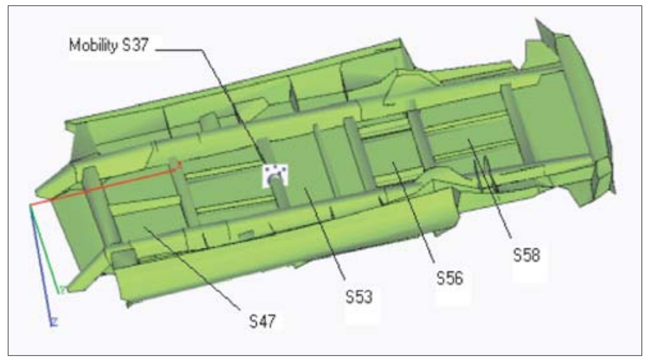


*Figure 10. Analytical autoSEA2 model.*

the 200-2000 Hz range – the first one for the 500 Hz 1/3 octave band and the second one for the 2000 Hz 1/3 octave. The two models respectively cover the 200-800 Hz range and the 500-2000 Hz range.

Few iterations of the Virtual SEA process were necessary to compute a robust sub-structuring. Figures 6 and 8 show these results on the "NVH meshes." A different color marks each SEA subsystem. Figures 7 and 9 present the respective AutoSEA1 model deduced from the two sub-structuring analysis and associated coupling schemes.

At 500 Hz the numerical tool predicts a structure divided into 13 SEA subsystems, whereas 14 subsystems are detected to model the minivan floor at 2000 Hz. The differences of sub-structuring clearly appear, and moreover it confirms that the number of subsystems increases with the frequency.

Before comparing experiments and Virtual SEA results, an analytical AutoSEA2 model was built from the initial finite element model with the knowledge of the optimal sub-structuring scheme. This model is shown on Figure 10, providing a clear view of the subsystem position.

The same DLFs have been used for both analytical and Virtual SEA modeling. Only two distinct DLFs were considered – one for the frame components and one for the panels. These DLFs both decrease as a constant power of the frequency.

Figures 11-14 present comparisons between the measurements, the AutoSEA2 results and the Virtual SEA results for the 4 panels indicated on Figure 10. Above 500 Hz, the deviation between the measurements and Virtual SEA results does not exceed 2 dB, whereas the AutoSEA2 results overestimate the measurements as soon as the frequency is low and the subsystems are far away from the excitation point.

Based only on the results of a numerical simulation, the Virtual SEA approach predicts the experimental data with acceptable differences.

**Trimmed Floor.** The second case consists in evaluating the effect of a trim on this minivan floor structure vibration. The objective of this test is to show that nearly the same structural SEA model can be used in both cases. The sound insulation covering only modifies the DLF of the panel. All other SEA

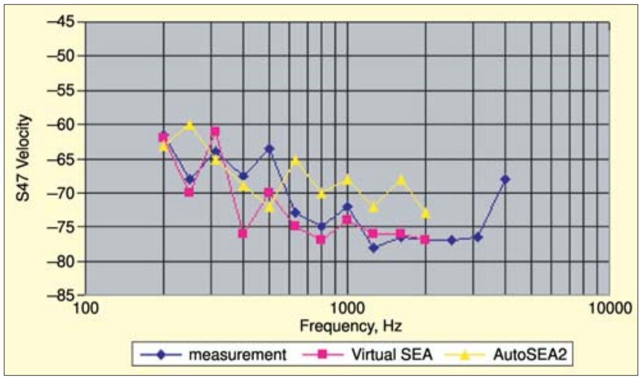


*Figure 11. Comparisons of velocity for subsystem S47.*

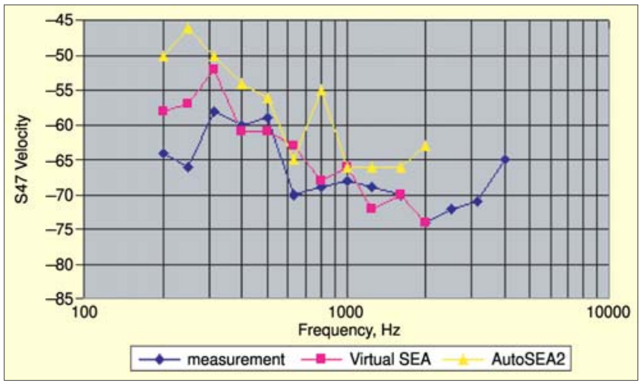


*Figure 12. Comparisons of velocity for subsystem S53.*

parameters (equivalent masses, CLF, etc.) are kept constant.

Figures 15-18 present the comparisons between the experimental data and the Virtual SEA predictions. Again, the effect of the trim on the vibratory behavior is well predicted by the Virtual SEA technique.

## Conclusion

The suggested method, called Virtual SEA, enables building a SEA model based on FEA results. A large, energetic transfer matrix is computed, providing a wide observation of the vibratory behavior of the studied structure. This matrix is then processed similarly to experimental SEA, in order to produce an 'optimized' SEA model of the studied structure. Such an SEA model allows some understanding of the medium/high frequency vibrations in terms of vibratory power flows between subsystems.

The main advantage of Virtual SEA is the quasi-automatic generation of SEA subsystems and Coupling Loss Factors. Virtual SEA does not require the a priori knowledge of the substructuring, which considerably reduces the required expertise and the associated manpower.

Virtual SEA was assessed in the case of a minivan floor. Computations and measurements were carried out separately and without interference, except for the damping estimation. An analytical SEA model was finally built to reflect today's practice. The Virtual SEA results are globally superior to the analytical SEA results. They follow the global trends at even the lowest frequencies and for subsystems distant from the source. The trimmed structure has also been modeled using the same SEA network, by increasing the damping of the panels. The prediction of the trim's effect on the floor vibrations is in good agreement with measurements.

This article has presented the current state of Virtual SEA, but numerous improvements can be expected. First, numerical simulation does not stop providing better and quicker results. The automatic sub-structuring that is not yet fixed will progress. Finally, stochastic computations could be naturally introduced, since the model identification process already considers input data uncertainties. This last improvement will be effective when the SEA software environment will support

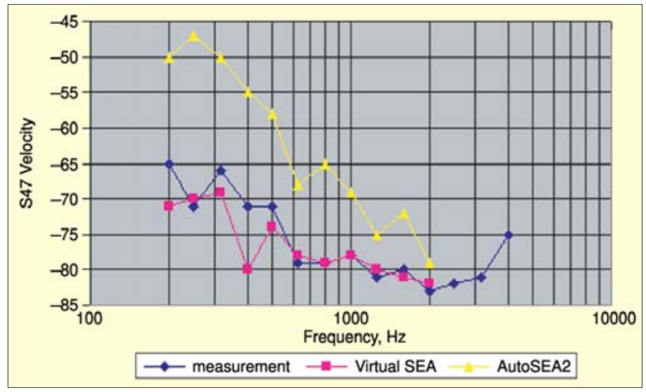


*Figure 13. Comparisons of velocity for subsystem S56.*

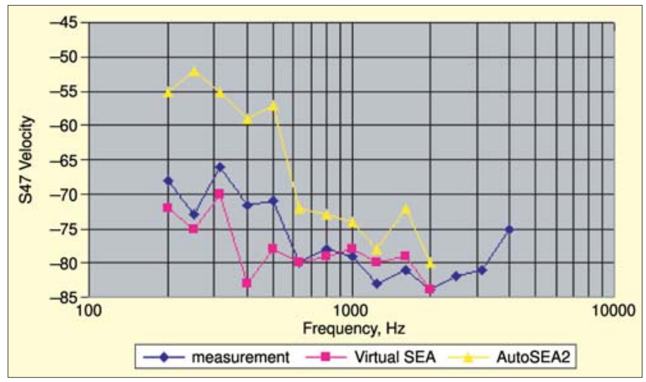


*Figure 14. Comparisons of velocity for subsystem S58.*

stochastic input data in order to provide probabilistic results.

Finally, there has been some concern that associated acoustic radiation problems have not been considered yet. It has been assumed that radiation problems will end up with a radiation efficiency determination. Numerous papers deal with radiation efficiencies, from FE computations to a simplified wave approach. Many solutions seem well suited to complete the proposed approach.

## References

1. Maxit, L. and Guyader, J.-L. "Estimation of SEA Coupling Loss Factors Using A Dual Formulation and FEM Modal Information, Part I: Theory and Part II: Numerical Applications," *Jnl. Of Sound & Vibration*, (2001) 239 (5) pp. 907-948.
2. Bouthier, O. and Bernhard R., "Models of Space Averaged Energetics of Plates," 1992, *American Institute of Aeronautics and Astronautics Journal*, 30, 616-623.
3. Langley, R. and Bremner, P., "A Hybrid Method for the Vibration Analysis of Complex Structural-Acoustic Systems," *Journal of the Acoustical Society of America*, 105(3), 1999, 1657-1671.
4. Le Bot, A., "A Vibroacoustic Model for High Frequency Analysis," *Journal Of Sound and Vibration*, (1998) 211 (4) pp. 537-554.
5. Zhao, X. and Vlahopoulos, N. "A Hybrid Finite Element Formulation for Mid-Frequency Analysis of Systems with Excitation Applied on Shord Members," *Journal of Sound and Vibration*, 200, Vol 237(2), pp181-202.
6. Simmons, C., "Structure-Borne Sound Transmission Through Plate Junctions and Estimates of SEA Coupling Loss Factors Using the FE Method," *Journal of Sound and Vibration*, 144, 215-227, 1991.
7. Finnveden, S., "Finite Element Techniques for Evaluation of Energy Flow Parameters," Proceedings of NOVEM 2000.
8. Soize, C., "Reduced Models in the Medium Frequency Range for General Dissipative Structural-Dynamics Systems," *European Journal of Mechanics*, A/Solids, Vol 17, No. 4, 1998
9. Meerbergen, K., "The Solution of Parametrized Symmetric Linear Systems and the Connection with Model Reduction," Technical Report KM-2000-2, Free Field Technologies, 16, place de l'Université, 1348 Louvain-la-Neuve, Belgium. Revised.
10. Bennighof, J. K., Kaplan, M. F., Muller, M. B. and Kim, M., "Meeting the NVH Computational Challenge: Automated Multi-Level Substructuring," Proceedings of the International Modal Analysis Conference XVIII, San Antonio, February 2000.
11. Mace, B. R. and Shorter, P. J., "Energy Flow Models from Finite Element Analysis," *Journal of Sound and Vibration* (2000), 233(3), 369-389.
12. Lyon, R. H., *Statistical Energy Analysis of Dynamical Systems*, MIT press, 1975.

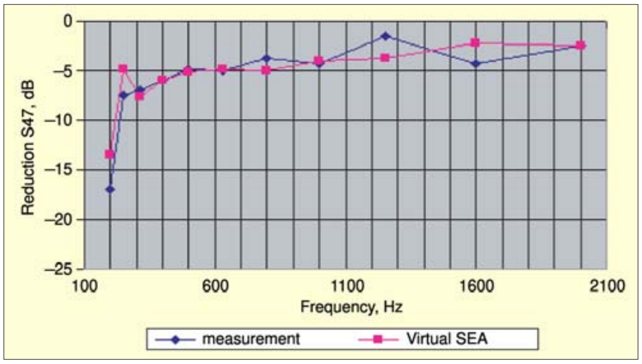


*Figure 15. Reduction velocity for subsystem S47.*

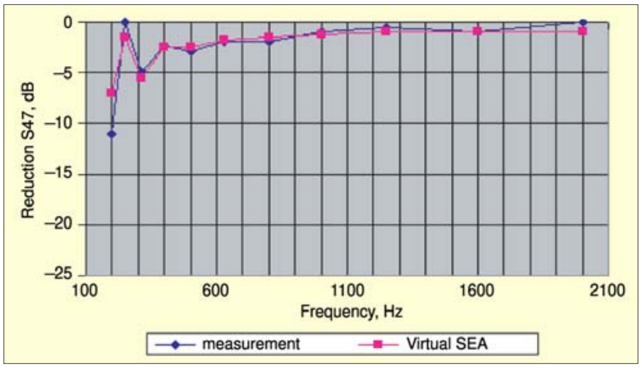


*Figure 16. Reduction velocity for subsystem S53.*

13. Lalor, N. "The Experimental Determination of Vibrational Energy Balance in Complex Structures," Paper 108429 Proc. SIRA Conf. on Stress & Vibn., London 1989.
14. SEA-XP User Guide Manual, InterAC Sarl, Version 2.5 , May 2004.
15. Rosen, M. and Borello, G., "Damping and Coupling Loss Factors Estimation in SEA Method: What is Really Measured ?," inter-noise 1996.
16. Cimerman, B. P., Bharj, T. and Borello, G., "Overview of Experimental Approach to Statistical Energy Analysis," Paper 97NV169, Proc. SAE Noise & Vibn. Conf. Traverse City, MI 1997.
17. Borello, G., "Identification of SEA Coupling Loss Factors on a Liquid Rocket Engine," inter-noise, 1991, Sydney, Australia.
18. Borello, G., "System Model of a High Speed Train Passenger Coach using SEA and Prediction in Working Conditions," inter-noise, 1995, Newport Beach, CA.
19. Borello, G., "Prediction and Control of Structure Borne Noise Transfers in Vehicles Using SEA," EURONOISE, October 4-7, 1998, Munich, Germany.

## Appendix – Experimental/Virtual SEA Model ID

The 'experimental' SEA process[13-15] is briefly reviewed here. Moreover, its application in Virtual SEA, which slightly differs from the previous, will be shown. The theoretical basis for the data reduction performed during the SEA model identification is described in the overview paper by Cimerman, Bharj and Borello.[16]

The virtually-derived SEA parameters are:

- Subsystem "equivalent" mass (volume).[16]
- Junction coupling loss factors $\eta_{jk}$ and $\eta_{kj}$.

Compared with experimental SEA, note that the Damping Loss Factor is known (input data) and that the input power is computed exactly.

In condensed form, the balance equation of the overall structure can be written as

$$\mathbf{LE} = \mathbf{P} \tag{A1}$$

where **L** is the loss matrix, **E** the energy vector and **P** the input power vector.

**Equivalent Mass Determination.** By considering the energy balance of the total studied system, the sum of the energies dissipated in each of the subsystems has to be equal to the power injected. In a frequency band centered on pulsation $\omega_0$, this energy balance result is expressed as:

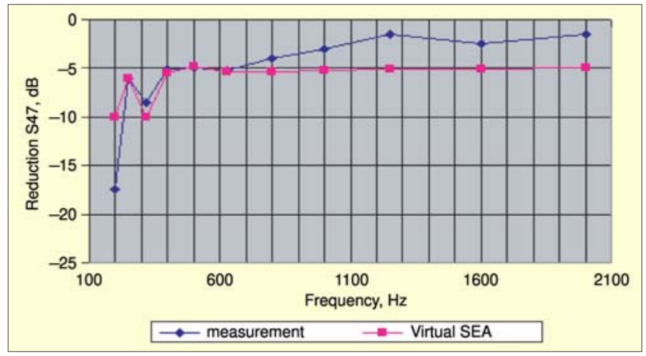


*Figure 17. Reduction velocity for subsystem S56.*

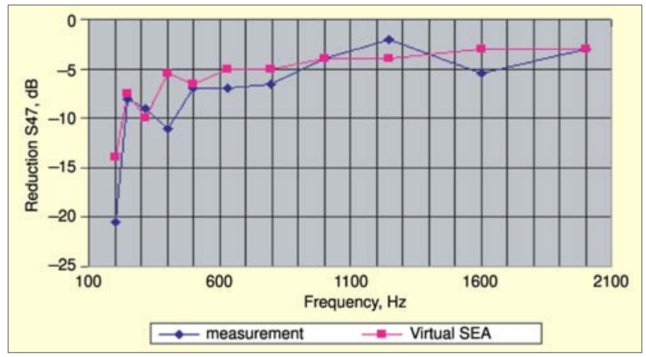


*Figure 18. Reduction velocity for subsystem S58.*

$$P_i = \sum_{j=1}^{N} \eta\omega E_{ji} \tag{A2}$$

where $P_i$ is the power injected at an excitation point in the substructure $i$ (computed), $\eta$ is the internal loss factor (input data), and $E_{ji}$ is the subsystem $j$ energy when subsystem $i$ is excited according to:

$$E_{ji} = M_j \left\langle \left| v_{ji} \right|^2 \right\rangle_{\Omega_j} \tag{A3}$$

where the quadratic velocity is estimated as:

$$\left\langle \left| v_{ji} \right|^2 \right\rangle_{\Omega_j} \cong \frac{1}{N_k} \sum_k v^2{}_{jik}$$

When each subsystem is excited, the following linear system can be derived from the balance Equation A2, invoking the uniform DLF, $\eta$, used in the computations and the Energetic Transfer Functions (Eq. 1):

$$\frac{1}{\eta\omega}\begin{pmatrix} 1 \\ \dots \\ 1 \\ \dots \\ 1 \end{pmatrix} = \begin{bmatrix} H_{11} & \dots & H_{N1} \\ \dots & & \\ \dots & H_{ji} & \dots \\ \dots & & \\ \dots & \dots & H_{NN} \end{bmatrix} \begin{pmatrix} M_1 \\ \dots \\ M_i \\ \dots \\ M_N \end{pmatrix} \tag{A4}$$

The vector of the equivalent mass is obtained by inverting matrix **H**:

$$\begin{pmatrix} M_1 \\ \dots \\ M_i \\ \dots \\ M_N \end{pmatrix} = \frac{1}{\eta\omega} \begin{bmatrix} H_{11} & \dots & H_{N1} \\ \dots & & \\ \dots & H_{ji} & \dots \\ \dots & & \\ \dots & \dots & H_{NN} \end{bmatrix}^{++} \begin{pmatrix} 1 \\ \dots \\ 1 \\ \dots \\ 1 \end{pmatrix} \tag{A5}$$

where the '++' superscript indicates a pseudo-inverse, provided matrix **H** is generally rectangular and numerous excitation points are used for each subsystem.

Note that the modal mass can be calculated without any assumption about the subsystem connection scheme. In addition, the energetic transfer matrix is well conditioned – the diagonal terms are indeed predominant.

In practice, Equation A5 can lead to negative equivalent masses in some 1/3 octave bands, the sign of inappropriate sub-structuring regarding the assumed energetic balance. That is, it does not exist in any physical SEA model based on the proposed sub-structuring. Compared to the previous application, the use of the automatic sub-structuring process in Virtual SEA almost provides positive answers. Nevertheless, specific inversion protocols are employed to avoid such non-physical results (Monte-Carlo methods[14]).

**Coupling Loss Factors (CLF) Determination.** Contrary to experimental SEA, where CLF can be computed independently from DLF, Virtual SEA requires the equivalent masses to be computed before the CLF. These masses are used to compute the Energy Transfer matrix using Equation A3.

The CLF calculation is performed from an analysis of exchanges between subsystems. The balance equation for subsystem $i$, subjected to excitation, is expressed as:

$$\frac{1}{\omega_0} = \left(\eta + \sum_{j \neq i}^{N_i} \eta_{ij}\right) M_i H_{ii} - \sum_{j \neq i}^{N_i} \eta_{ji} M_j H_{ji} \tag{A6}$$

For subsystem $k$, where no excitation applies, the balance equation is:

$$0 = \left(\eta_k + \sum_{j \neq k}^{N_i} \eta_{kj}\right) M_k H_{kk} - \sum_{j \neq k}^{N_k} \eta_{jk} M_j H_{jk} \tag{A7}$$

$N_i$ and $N_k$ represent the total number of couplings between element $i$ and element $k$ as defined in the coupling scheme.

These balance equations consist of a set of $N$ linear equations, one for each excited sub-system. Applying a load successively on each subsystem leads to a total of $N*N$ equations, involving all CLF. This linear system is solved using the condensation technique proposed by Lalor,[13] which transforms the coupling coefficient calculation into a successive resolution of smaller linear systems with size $N_{i-1}$. $N_i$ is the number of subsystems that are coupled to subsystem $i$, according to the coupling scheme.

The final expression of the CLF, describing the coupling between subsystem $i$ and the $N_{i-1}$ connected subsystems appears as:

$$\begin{pmatrix} \cdots \\ \eta_{ki} \\ \cdots \end{pmatrix}_{\substack{k \in \{\alpha, N\}, \\ k \neq i}} = \begin{bmatrix} \frac{E_{\alpha\alpha}}{E_{i\alpha}} - \frac{E_{\alpha i}}{E_{ii}} & \cdots & \frac{E_{N_i \alpha}}{E_{i\alpha}} - \frac{E_{N_i i}}{E_{ii}} \\ \cdots & \frac{E_{kk}}{E_{ik}} - \frac{E_{ki}}{E_{ii}} & \cdots \\ \frac{E_{\alpha N_i}}{E_{iN_i}} - \frac{E_{\alpha i}}{E_{ii}} & \cdots & \frac{E_{N_i N_i}}{E_{iN_i}} - \frac{E_{N_i i}}{E_{ii}} \end{bmatrix}^{-1} \begin{pmatrix} \frac{P_i}{\omega_0 E_{ii}} \\ \frac{P_i}{\omega_0 E_{ii}} \\ \frac{P_i}{\omega_0 E_{ii}} \end{pmatrix} \tag{A8}$$

This problem has to be solved for each SEA subsystem in order to get the total set of CLFs needed by the proposed coupling scheme.

This system of equations can produce a few negative CLF values in some frequency bands, indicating that the proposed model (including the coupling scheme, estimated subsystems energy and SEA assumptions) is not physical. This difficulty is overcome first by taking advantage of the multiple excitations of each subsystem and formulating a least square problem, and second by using a Monte-Carlo inverse process as mentioned to determine the equivalent masses.

Again, the use of the automatic sub-structuring technique greatly improves the identification process. S/V

The authors can be contacted at info@interac.fr.